Multiscale analysis of nitrogen adsorption and desorption isotherms in soils with contrasting parent materials and texture

[1]Jorge Paz-Ferreiro, [2]Mara de Andrade Marinho, [3]Cleide A. de Abreu and [4]Eva Vidal Vázquez

[1] Royal Melbourne Institute of Technology University, School of Civil, Environmental and Chemical Engineering, Melbourne, Australia.

[2] Faculdade de Engenharia Agricola (FEAGRI), Universidade Estadual de Campinas (UNICAMP), Av. Candido Rondon, 501, Campinas, 13083-875, SP, Brazil.

[3] Instituto Agronômico de Campinas (IAC), Av. Barão de Itapura, 1481, Campinas, 13020-902, SP, Brazil.

[4] Facultad de Ciencias, Universidade da Coruña, Campus de Elviña, sn. Coruña, Spain.

Corresponding author: jpaz@udc.es

Abstract

Soil specific surface area (SSA) is as an important soil property, which is strongly related soil texture, clay type and colloidal components. Most frequently, SSA is estimated admitting a non-fractal model, from adsorption isotherms, in a limited range of relative pressure. On the other hand, fractal and multifractal approaches have been used to describe Nitrogen adsorption and desorption isotherms (NAIs and NDIs, respectively), measured over the full range of relative preassures. Soil profiles developed either over sandstone, or over weathered (basic or clayey) parent material were sampled at neighbouring sites. The two studied soil groups showed significant differences in texture , CEC and SSA. As in previous studies, the scaling properties of both nitrogen adsorption and desorption isotherms from all the studied soil horizons

could be fitted reasonably well with multifractal models. During adsorption, parameter (D_{-5}-D_5) was significantly greater for heavily textured soils than for medium textured soils. Meanwhile during desorption there were no significant differences in mean values of (D_{-5}-D_5). Parameters D_{-5}, D_1, D_2 and D_5, showed greater values for clayey soils during adsorption, but during desorption the trend was opposite and all of them were higher for medium textured soils. These results suggest that the measure is more evenly distributed during adsorption for clayey soils and during desorption for medium textured soils. These differences are consistent with a wider hysteresis loop of the medium texture soils compared to that of the clayey soils. Several multifractal parameters extracted from NAIs and NDIs also were useful to distinguish between clayey and medium textured soils.In opposite to results from previous work, there was no significant relationship between multifractal parameters from NAIs, and NDIs and soil textural fractions or organic carbon content.

Introduction

The quality of a soil, defined as its ability to perform a given function or its suitability for chosen uses in agroecosystems, depends both on inherent or dynamic soil properties (Doran and Parker, 1994; Carter et al., 1997, Lal, 1998). Inherent soil properties such as particle size distribution, particle density, or soil mineralogy rely upon soil-forming factors, whereas dynamic soil properties, such as aggregate stability, water and nutrient status, bulk density change in response to soil use and management (Carter et al., 1997), bur also may be affected by inherent soil properties. Several properties such as organic matter content, specific surface area or bulk density may be considered as inherent properties for deep horizons, but have been shown to be dynamic, or use dependent, near the soil surface.

Soil mineral fraction is most frequently characterized by particle size analysis, because soil texture greatly influences the physical and chemical processes, which affect soil functions. Also, many macro-scale physical and chemical soil properties are closely related to grain-scale properties such as surface area, porosity, pore size distribution, pore geometry and energy distribution (Petersen et al., 1996, Hajnos et al., 2000). In particular, specific surface area (SSA) is commonly considered as an important soil property which is strongly related soil texture, clay type and colloidal components.

The usual procedure for determining soil surface properties is through analysis of adsorption-desorption isotherms, plotted against the relative pressure (p/p_o) in the range $0<p/p_o<1$, at constant temperature. The most common adsorbate used to measure adsorption and desorption isotherms is Nitrogen (Rouquerol et al., 1999). In general, nitrogen sorption isotherms are merely used to determine the specific surface area of a soil using the well-known Brunauer-Emmet-Teller (BET) model (Brunauer et al., 1938). This is because soil SSA has been proven to be a useful parameter, which has been correlated with important soil properties such as clay and sesquioxides content, clay type, CEC, retention and release of chemicals, available water, swelling-shrinking, aggregate stability, etc. (Petersen et al., 1996; Feller et al., 1992; Jozefaciuck et al., 2006; Hepper et al., 2006; Bartoli et al., 2007; Paz-Ferreiro et al., 2009).

Fractal-based models have been in the past used to describe soil NAIs (Pachepsky et al., 1995; Hajnos et al., 2000; Jozefaciuk et al., 2006). Also, the scaling properties of NAIs from soils and artifitial organoclays have been reasonably well described by multifractal models, (Paz-Ferreiro et al., 2009, 2010, Vidal-Vazquez and Paz-Ferreiro, 2012; Lado et al., 2013). More recently, Paz-Ferreiro et al., 2013 performed multiscale analysis of both NAIs and NDIs. Comparison of results cropped from the classical BET model and those from multifractal approaches is not straightforward. First, the BET model, estimates the total surface area from adsorption isotherms in a limited range of relative pressure, (i.e., $0.05 < p/p_0 < 0.35$), while fractal and multifractal approaches use the information contained in the entire adsorption or desorption curve. Second, the BET method assumes that the soil pore-solid surface is not a fractal. Nevertheless, it has been claimed that SSA and scaling analysis of N_2 isotherms yield complementary information that may be useful for a better understanding of the geometry of soil surfaces and porous systems (Paz-Ferreiro et al., 2013).

Previously, multifractal analysis of NAIs (Paz-Ferreiro and Vidal Vázquez, 2012) and both, NAIs and NDIs (Paz-Ferreiro et al, 2013) has been performed in Brazilian soils, collected in Minas Gerais and Santa Catarina states, respectively. For the present study, soil profiles, developed over sandstone, and weathered material from clay sediments and basic parent material, with contrasting texture were sampled in neighbouring sites of São Paulo State, Brazil. Parent material and topography are the main soil-forming factors that explain soil distribution at the local scale in São Paulo state (Oliveira et al., 1979; IPT, 1981, 1997), where the main soil types are Oxisol and Ultisol (Oliveira et al., 1979). These soil over sandstone and weathered (mainly basic) materials are well known for their contrasting pedogenic origin, physical chemical and biological properties, susceptibility to erosion and quality (Weill and Sparovek, 2008). Understanding the inherent properties of these soils helps to protect the environment quality and at the same time makes agriculture sustainable. Therefore, the aims of this study were: i) to evaluate SSA in the sampled soils, and to assess its dependence on general soil properties ii) to examine patterns of multifractal property exhibited by NAIs and NDIs for the soils with contrasting texture and properties studied and iii) to compare the performance of multifractal parameters and general soil properties, including SSA, for distinguishing between the studied soil groups.

Materials and Methods

Site characteristics and soil sampling

The study was conducted at the region of Campinas, São Paulo State, Brazil. Site altitudes ranged from 574 to 640 m above see level. According to Köppen the local climate is a transition between two mesotermic types, those with dry winter (Cwa) and hot summer (Cfa). Mean annual temperature in Campinas is 22.4^{o}C and a mean yearly precipitation 1382 mm.

Six soil profiles were selected and sampled; three of them were developed over sedimentary rocks (sandstone and siltstone), one was over loamy-clayey sediments and the two other were over basic rocks (diabase). Table 1 lists depth of the 32 horizon collected from the 6 soil profiles, main site characteristics (location, parent material) and classification, following the Brazilian System of Soil Classification, BSSA, described by EMBRAPA (2006), Soil Survey Staff, SSS (2010) and World Reference Base, WRB, (2006). Soil profiles nº 1 to 5 were sampled in municipalities neighboring to Campinas (namely Monte Mor and Sumaré), while profile nº 5 was sampled at the experimental farm of the College of Agricultural Engineering, State University of Campinas (FEAGRI-UNICAMP). Location of profiles 1 to 5 can be seen as Supplemental Digital Content, Figure S1.

Profiles 1, 2 and 3, (in short P1, P2 and P3), collected at Monte Mor Municipality, were developed over fine sandstone and siltstone materials from the Tubarão formation (Upper Carboniferous), and they belong to a toposequence developed along a hillside on undulate to strong undulate relief. P1 was located on the lower steep hillside and it was classified as an Entisol, while P2 and P3 were sampled at the middle and upper hillside, respectively and classified as Ultisols (i.e. Hapludults, SSS, 2010).These soils were devoted to extensive pasture. Typically they are characterized by a high erodibility index; the high susceptibility to water erosion, which is enhanced by the undulated relief and by the presence of a lithic contact (P1), or a textural gradient (P2) that may be abrupt (P3)

Profiles 4 and 5 (in short P4 and P5), collected at Sumaré Municipality, were developed on strongly weathered deposits derived from loamy-clayey sediments and diabase materials, respectively, on a smooth undulated relief. Profile P4, classified as an Oxisol (i.e. Hapludox) was on the flatter plateau at the top of the hillside, while P5, classified as an Ultisol (i.e. Rhodudult), equivalent to Nitisol in the WRB was on slope position of the middle hillside. The else soil profile, P6, was also over weathered diabase on a smooth slope position and it was classified as an Oxisol. P4 and P5 were cropped to sugar cane, while P6 was used for crops in rotation. Oxisols and Rhodudults (Nitosols) are considered as stable and resistant to erosion (Weill and Sparovek, 2008).

Analysis of general soil physical and chemical properties

Soil samples were ground to pass through 2 mm sieve. For each horizon collected, clay, silt and sand content was measured by the sieve-pipette method (EMBRAPA, 1997). Determinations of pH, organic carbon content, exchangeable bases (Ca, Mg K) and exchangeable acidity (H + Al) were conducted as described in van Raij et al., (2001). For each sample, cation exchange capacity (CEC), sum of bases (SB) and percent base saturation (V %) were calculated from the respective exchangeable cations.

N_2 isotherms and soil specific surface area

Determinations of nitrogen adsorption and desorption isotherms were obtained in A Soptomatic 1990 equipment manufactured by Thermo Finnigan (Milano, Italy). Two replicate measurements per horizon were performed in small aggregates. The inert gas used (N_2) was 99.998% pure and determinations were performed at the liquid state (77 K temperature). Details about sample preparation and NAI and NDI determination procedure have been previously described (Paz-Ferreiro et al., 2013). Adsorption isotherms were acquired in a scale of relative pressures, p/p_0, ranging from 0.001 to about 0.997 (as in Paz-Ferreiro et al., 2009; Vidal-Vazquez and Paz-Ferreiro, 2012). The scale used for desorption isotherms was from the highest relative pressure of about 0.997 to lowest p/p_0 values near 0.01 (as in Paz-Ferreiro et al., 2013).

The soil SSA was obtained from the adsorption branch of the isotherms using the BET model (Carter et al., 1986). The BET model easily estimates the total surface area, since the area covered by a single molecule adsorbed on the soil surface is known; assuming implicitly that surface and pore geometry is Euclidean (Rouquerol et al., 1999; Bartoli et al., 2007, Paz-Ferreiro et al., 2013). Figure 1 shows examples of absorption-desorption isotherms from selected horizons over sandstone and weathered materials.

Multifractal analysis

The method of moments (Halsey et al., 1986) and the direct method (Chhabra and Jensen, 1989) were employed here to perform multifractal analysis of NAIs and NDIs. This procedure has been frequently used for multifractal evaluation of various soil properties, including pore size distributions (Posadas et al., 2003; Tarquis et al., 2006), Particle size distributions (Miranda et al., 2006) surface roughness (Vidal Vázquez et al., 2008) etc. Also, more recently it has been employed for assessing multifractal property of either the adsorption branch (Paz-Ferreiro et al., 2009, 2010; Vidal-Vázquez and Paz-Ferreiro, 2012; Lado et al., 2013) or both, the adsorption and desorption branches of nitrogen isotherms. Therefore multifractal concepts and method of analysis will be here only briefly described.

Cumulative adsorption and desorption data sets are taken as raw data, from which differential change of N_2 volume, Δn, for each p/p_0 interval can be computed. Therefore, the distributions of N_2 was taken as the measure, μ_i, and the relative pressure, p/p_0, itself, as the scale, δ (Paz Ferreiro et al.; 2009, 2013). Thereafter, the data sets consisting of distributions of N_2 during absorption or desorption are normalized, meaning that a new variable, the probability mass function, p_i (δ) or $\mu_i(\delta)$, is defined as:

$$p_{ii}(\delta) = \mu_i(\delta) = \frac{N_i(\delta)}{N_t}, \qquad (1)$$

where N_i (δ) is the value of the measure in the i^{th} segment of scale δ in a p/p_0 interval and N_t represent the total mass in the whole scale of applied relative pressure .

Multifractal analysis of the probability mass function yields the following functions: mass exponent function, τ_q, generalized dimension, D_q. and singularity spectrum, $f(\alpha)$ versus α. First, a partition function, $\chi(q,\delta)$, was estimated from the $p_i(\delta)$ values as defined as: $\chi(q,\delta) = \sum_{i=1}^{n(\delta)} \mu_i^q(\delta)$, where $n(\delta)$ is the number of intervals covering the p/p_0 scale and q is the order of the statistical moment. The partition function scales with the box size, δ, as:

$$\chi(q,\delta) \propto \delta^{-\tau(q)} \qquad (2)$$

where $\tau(q)$ is the mass exponent or scaling function of order q.

The scaling function τ_q is also related to the generalized dimension D_q, Therefore, multifractal sets can also be characterized by their spectrum of generalized dimensions using the following relationships:

$$D_q = \lim_{\delta \to 0} \frac{1}{q-1} \frac{\log[\chi(q,\delta)]}{\log \delta} = \frac{\tau_q}{(1-q)}, \ q \neq 1 \qquad (3a)$$

$$D_1 = \lim_{\delta \to 0} \frac{\sum_{i=1}^{n(\delta)} \mu_i(\delta) \log[\mu_i(\delta)]}{\log \delta}, \ q = 1 \qquad (3b)$$

The generalized dimensions, D_q for q = 0, q = 1 and q = 2, are known as the capacity, the information (Shannon entropy) and correlation dimensions, respectively. The spectra of generalized dimensions for different q have specific features for multifractals (i.e. $D_0 > D_1 > D_2$), while for monofractals D_q is a constant.

The singularity spectrum, f(α), and the coarse Hölder exponent, also known as local scaling index, α_q, can be estimated from the mass exponent function, τ_q through a Legendre transformation. However, this procedure is not straightforward, and most frequently f(α) and α have been obtained by the direct method.

The direct method (Chhabra and Jensen, 1989) employs the scaling properties of another normalized variable, and is based on the contributions of individual segments to the partition function, $\mu_i(q,\delta)$, that is defined as:

$$\mu_i(q,\delta) = \mu_i^{\,q}(\delta) / \sum\nolimits_1^{n(\delta)} \mu_i^{\,q}(\delta) . \qquad (4)$$

Now, using a set of real numbers, $-\infty < q < \infty$, the functions $f(\alpha)_q$ and α_q can be computed as follows::

$$f\left(\alpha(q)\right) \propto \frac{\sum_{i=1}^{N(\delta)} \mu_i(q,\delta) \log\left[\mu_i(q,\delta)\right]}{\log(\delta)} \qquad (5a)$$

$$\alpha(q) \propto \frac{\sum_{i=1}^{N(\delta)} \mu_i(q,\delta) \log\left[\mu_i(\delta)\right]}{\log(\delta)} \qquad (5b)$$

As before stated, the scale of experimental NAI and NDI curves was in the range of relative pressures: $0.001 < p/p_0 < 0.997$ and $0.01 < p/p_0 < 0.997$. The first points of the scale were accepted as similar for adsorption and desorption phases. Using this rule, the number of experimental data points of N_2 volume versus relative pressure (p/p_0) was between 41 and 52.

Linearity of these log-log plots of the normalized measures $\chi(q,\delta)$ versus measurement scales, δ, was found for successive partitions from $1< k < 4$, as in a previous study (Paz-

Ferreiro et al., 2009). For k < 1, however, the double logarithm plots departed from linearity. Generalized dimension spectra, D_q, were calculated with Eq. (6) in the moment range $-5 \leq q \leq 5$ at 0.5 lag increments. Values α and $f(\alpha)$ of the singularity spectrum were calculated using Eq. (5). Points (α, $f(\alpha)$) were accepted in the singularity spectrum only if the logarithm of the normalized measures varied linearly with the logarithm of the measurement scale, which means regressions with coefficients of determination, $r^2 \geq 90$. Subsequently, Several parameters were obtained form the generalized dimension spectra for successive *q* moments (i.e., D_5, D_0, D_1, D_2, D_{-5}) and the singularity spectra (i.e α_0 or Hölder exponent of order zero).

Statistical analysis

One way ANOVA was performed to compare general properties and multifractal parameters among soil groups. Differences between mean values of these variables at the $P<0.05$ level were tested using the Fisher Least Significant Differences (LSD) procedure and the Tukey test.

Principal component analysis (PCA) was performed taken into account on the one hand data sets with soil physico-chemical properties, and on the other hand these properties together with several multifractal parameters. All the raw data were standardized for mean 0 and variance 1 and PCA was performed in the resulting data matrix. The three first principal components (PC1, PC2 and PC3) were selected for the ordination of cases.

Product-moment correlations were performed between soil physico-chemical properties, multifractal parameters and the scores on the PC1, PC2 and PC3 for the interpretation of the new axis. Statistical analyses were performed using SAS scientific software, version 8.0 (SAS, 1999).

Results and discussion

General soil physico-chemical and surface properties

General soil physical and chemical properties of the studied soils are listed in Table S1 of the Supplementary Digital Content. Profiles 1 to 3, over sandstones, were loamy and sandy loam textured, while profiles 4 to 6, over basic rocks and sediments were clayey textured, except for the top horizon of profile 4, which was sandy clay. Clay content in the former group of soil profiles was lower than 225 mg kg^{-1}, whereas it was higher than 384.5 mg kg^{-1} for the latter group. For simplicity, these two soil groups with contrasting clay contents will be next referred to as medium textured and clayey soils.

Organic matter contents for medium textured and clayey soils ranged 16-37 g kg^{-1} and 16-31 g kg^{-1}, respectively. Soils over sandstone had pH values from 4,1 to 4.9, while the counterpart ranged 4.1-5.6. The two groups of soils studied were characterized by low CEC values, (< 13 $Cmol_+$ kg^{-1}). This notwithstanding CEC was much higher for clayey soils over weathered materials than for medium textured soils over sandstone, and this trend was also observed for Al + H. However, exchangeable K, Mg, Mg as well as sum of exchangeable bases, SB and percent base saturation showed similar values in these two soil groups; SV values were rather scarce (< 4 $Cmol_+$ kg^{-1}) in the two soil groups.

Differences in nitrogen isotherms of the two soil groups are noteworthy, as shown in Figure 1. The cumulative volume of N_2 adsorbed was about 15 times higher for the clayey horizon, compared to the loamy horizon. The hysteresis loop, however, was wider in the loamy horizon.

Values of SSA were in the range from 2.86 to 47.26 m^2g^{-1}. Parallel with clay content, SSA was below 15.09 m^2 g^{-1} for medium textured soils, and above 26.21 m^2 g^{-1} for clayey soils (Figure 2). Overall, clay content and soil SSA showed a very strong correlation ($r > 0.99$, $P<0.01$, see also Table 1). The regression equation between SSA and clay content for our studied soils was: SSA = 0.75 clay -1.26.was quite similar to that proposed by Feller et al. (1992) for tropical soils. However, SSA values of soils from São Paulo in this study are lower than those reported fro soils from Minas Gerais (Vidal Vázquez and Paz-Ferreiro, 2010) and Santa Catarina (Paz-Fereiro et al., 2013). Moreover, no significant relationship was found between these soil SSA and properties of the soil exchange complex (CEC, SB or exchangeable cations). The association between SSA and CEC has been proved for soils from temperate climates (Petersen et al., 1996; Hepper et al., 2006; Paz-Ferreiro et al., 2009). Highly weathered soils from the tropics however, are identified by a clay fraction made not only of clay particles but also rich in iron and aluminium oxides and hydroxides (Feller et al., 1992). These secondary constituents present in the clay fraction may contribute to SSA but are not able to develop significant CEC.

ANOVA analysis showed significant differences ($P<0.05$) between the two groups of soils studied, P1 to P3 versus P4 to P6 (i.e. medium textured versus clayey soils) for means values of texture fractions (sand, silt and clay), SSA, CEC and H+Al, while mean values of pH, organic matter content, SB and V were statistically similar.

Multifractality of adsorption and desorption isotherms

Because partition functions have been estimated in the range of linear behaviour, involving segment sizes limited to $1< k <4$, the range of log (δ)employed in this study was between 0.30 and 1.40. Partition functions in our work similar to those shown in Paz-Ferreiro et al. (2009) and Vidal Vázquez and Paz Ferrero, (2012).

Table 3 list various multifractal parameters (D_5, D_2, D_1, D_{-5}) extracted from the generalized dimension function and from the singularity spectrum, $f(\alpha)$ versus α, of adsorption isotherms of the studied soils. Table 4 lists the respective parameters for desorption isotherms. Examples of D_q versus q functions are shown in Figure S2 as Supplementary Digital Content.

The generalized dimension spectrum, D_q, of all the studied adsorption and desorption isotherms showed a non-linear trend, so that they were rather sigma shaped curves. The shape and the steadily decreasing trend of the generalized dimension, D_q, when q moves from -5 to +5, and the ranking of the three first positive moments, i.e., D_0, > D_1 > D_2 suggests multifractal behavior of all the adsorption and desorption isotherms studied.

The entropy dimension, D_1, has been recognized as a measure of diversity and in our study case gauges the concentration degree of N_2 adsorption or desorption on a specific p/p_0 interval. When D_1 approaches D_0 ($D_0 = 1$), the measure is considered to be evenly distributed over all the scale measured, while D_1 values close to zero reflect the measure concentrates in a small size domain of scale (Halsey et al., 1986; Tarquis et al., 2006; Vidal Vázquez et al., 2008). Entropy or information dimension, D_1, of the 32 horizons studied (two repetitions per horizon) varied between 0.492 and 0.643, with a mean value of 0.570, for adsorption isotherms, (Tabla 3) and between 0.620 and 0.797, with a mean value of 0.683, for desorption isotherms (Table 4). Figure 5 shows the relationship between D1 values extracted from NAIs and NDIs .Mean values for NAIs and NDIs were significantly different ($P<0.05$). Lower values of D_1 for adsorption isotherms compared with desorption isotherms are consistent with previous work (Paz-Ferreiro et al., 2013). The smaller the value of D_1 is, the higher the measure is concentrated in a small size domain of the studied scale. Both, nitrogen adsorption and desorption isotherms are sharper at the end of the curve (Figure 1), where the measure, in this case cumulative nitrogen volume, is subjected to rapid increases. However, adsorption changes by condensation is more abrupt than desorption changes by evaporation, because of the hysteresis loop. Hence, the measure is more evenly distributed for desorption than for adsorption isotherms.

The correlation dimension, D_2, showed a trend to decrease as D_1 decreased, although there were differences in the extent of the (D_1 - D_2) values, exhibiting various degrees of multifractality for adsorption and desorption isotherms.

Examples of f (α)-α) spectra for adsorption and desorption isotherms of medium and heavily textured soils are shown in Figure 3 and Figure 4, respectively. The singularity spectrum of all the studied nitrogen isotherms were concave down parabolic curves. Again, shape and asymmetry of the singularity spectra showed the scaling properties of NAs and NDIs could be fitted reasonably well with multifractal models.

All the spectra were asymmetric, left-deviating curves, shorter toward the right and more or less longer toward the left; Thus, there were various degrees of asymmetry in the studied data sets. Asymmetry of the f (α) spectrum toward the left indicates domination of high or presence of extremely high values in the probability distribution of the measure. Rare high events in N_2 adsorption and desorption were more frequent than rare low events. Hence, the general shape of the (α) spectra from adsorption and desorption isotherms is compatible with the rapid changes during N_2 condensation (at the adsorption phase) or evaporation (at the desorption phase) recorded for high relative pressures, i.e. , p/p_0 values approaching the unity.

The amplitude of the f(α) spectrum is an indicator of heterogeneity, because it provides information on the diversity of he scaling exponents of a measure. So, the wider the f(α) spectrum is, the higher is the heterogeneity in the scaling indices. Also the width of the generalized dimension spectra, which can be assessed by the difference (D_{-5}-D_5) can be considered as a measure of heterogeneity. Following these criteria, desorption isotherm have been demonstrated more homogeneous than adsorption isotherms.

Values of Hölder exponent of order zero, α_0, extracted form the singularity spectra of adsorption and desorption isotherms also are reported in Table 3 and 4, respectively. Parameter α_0, quantifies the average degree of mass density of the measure. The α_0, values varied between 1.260 and 1.579 for adsorption isotherms and between 1.113 and 1.257 for desorption isotherms. These figures are relatively high and of the same order of magnitude as reported before for NAIs and NDIs (Paz-Ferreiro et al., 2009; Vidal-Vázquez and Paz-Ferreiro, 2012; Paz-Ferreiro et al., 2013). Opposite to entropy dimension, D_1, Parameter α_0, was higher for adsorption than for desorption isotherms. The relatively large values of exponent α_0 and the smaller amplitude of NAI curves compared to NDI curves are compatible with a higher heterogeneity and a lower anisotropy of the distribution of the measure during adsorption.

Summarizing, low D_1 values reflect the fact that most of the measure concentrates in a small size domain of the study scale, while high values of D_1 indicate that the measure is evenly distributed. Low D_2 means a small spatial autocorrelation and vice-versa. Moreover, large α_0 and wide (D_{-5}-D_5) are characteristic of a high heterogeneous measure. Hence, adsorption isotherms behaved as more clustered (i.e. less evenly distributed) measures, with lower entropy , D_1, and correlation, D_2, dimensions, higher heterogeneity and, in general, lower asymmetry, when compared with desorption isotherms. The multifractal parameters gave a good description of how the amount of N_2 gas rises and recedes in the absorption and desorption isotherms, respectively, in the scale range $0< p/p_0<1$.

Multifractal parameters and parent material or texture

Mean values of several multifractal parameters extracted from NAIs and NDIs are listed in Table 5, where .one-way ANOVA analysis results are also shown. Parameters D_{-5}, D_2, D_5, (D_{-5}-D_5) and α_0, extracted from multifractal curves of NAIs were significantly different between the two contrasting groups of soils studied, while D_1 during absorption showed not significant differences ($P<0.05$). On the other hand, parameters D_{-5}, D_1, D_2, D_5 from the generalized dimension function of desorption isotherms showed also significant differences, (D_{-5}-D_5) while α_0 during desorption was not significantly different ($P<0.05$) between these soil groups.

Heterogeneity, given by parameter (D_{-5}-D_5) was significantly greater for heavily textured, over weathered materials, than for medium textures soils, over sandstone during adsorption ($P<0.05$). Meanwhile during desorption there were no significant differences in mean values of (D_{-5}-D_5), but these were slowly higher for soils over sandstone.

Parameters D_{-5}, D_1, D_2 and D_5, showed greater values for clayey soils during adsorption, but during desorption the trend was opposite and all of them were higher for the medium textured soils. This result suggest a more evenly distributed measure of the clayey soils and medium textured during adsorption and desorption, respectively.. These differences are consistent with the wider hysteresis loop of the medium textured soils compared to that of the clayey soils.

Hölder exponent of order 0 was higher for soils over weathered materials compared to those over sandstone, both for NAIs and NDIs. However differences between these two soil groups were significant ($P<0,05$) for adsorption isotherms, and not for desorption isotherms.

Multifractal parameters and general soil properties

Pearson product moment correlations between selected multifractal parameters (D_{-5}, D_2, D_5, (D_{-5}-D_5) and α_0), and organic carbon content and play content showed in general no significant differences; the only exception was the relationship (D_{-5}-D_5) during the desorption phase versus organic matter content, which were positively correlated (R^2 =

0,391). This is not consistent wit the results of previous work (Paz-Ferreiro et al:, 2013), which demonstrates that scaling heterogeneity showed a trend to increase as a function of clay content and to decrease as a function of organic carbon content, both for NAIs and NDIs. Our results, however suggest that clay and organic carbon are not factors determining the geometrical heterogeneity at the surface-pore interfaces of the studied soils. In other words, the nonlinearity of NAIs and NDIs of soils collected in Santa Catarina (Paz-Ferreiro et al; 2013) and in Saão Paulo) may be driven by different soil properties or processes. This reinforces the need to further perform multifractal analysis of N_2 isotherms.

Principal component analysis (PCA) was used to further asses the relationships between general soil properties and multifractal parameters. Results of PCA performed for two datasets, which included physicochemical properties and parameters resulting from multifractal analysis (D_1, D_2 and α_0) of either absorption or desorption isotherms, are shown as Supplementary Digital Content (Table S2).

For the two data sets consisting of general soil properties and multifractal parameters from either NAIs or NDIs, the main contributions to the first axis were from pH, some properties of the exchange complex and sand content. So, pH, SB and V (%) were best positively and sand content and exchangeable Al best negatively correlated to the scores of PC1, respectively ($r \geq |0.74|$, $P < 0.001$). Other various soil properties were also correlated to PC1 scores: clay content, exchangeable H + Al and SSA, but showed higher dispersion ($P<0.01$), meaning its contribution was much lesser.

The scores of the second axis were significantly ($P > 0.05$) and positively correlated to clay content, H+Al, CEC, V (%) and SSA, while they exhibit negative correlations with silt and sand contents. Best correlated variables ($r \geq |0.74|$, $P < 0.001$) were SSA, silt and clay contents. Multifractal parameters also might contribute or not to the second axis. So, for adsorption isotherms D_2 and α_0 were positively correlated (r= 0.429 and r = 606 for the former and the latter, respectively) with the scores of PC2. However, parameters extracted from desorption isotherms showed stronger correlation with PC2 scores (r= - 730, r= -760 and r = 606 for D1, D_2 and α_0, respectively).

In the orthogonal space defined by PC1 and PC2, this second axes clearly separates profiles P1 to P3 from profiles P4 to P6 (Supplementary Digital Content Figure S3). Therefore, PCA showed soil surface properties, such as SSA obtained by classical methods, and multifractal parameters were also useful to associate soil profiles with similar properties.

Realistic values of SSA have proven to be of great interest in several application related to soil environmental quality (Pachepsky et al., 1995; Petersen et al., 1996; Hajnos et al., 2000). The two studied soil groups from São Paulo State significantly differed in texture (clay, silt and san content), CEC and SSA. Sandy-loam and loamy soils with low SSA from undulated landscapes are most susceptible to clay dispersion, seal formation and heavy soil erosion. Clayey soils with relatively high SSA from stable landscapes exhibit a high aggregate stability and infiltration rate and they are less susceptible to erosion. Also the former and more erodible soils are expected to exhibit high enrichment ratios for sediment, and associated nutrients and contaminants than the latter stable soils.

Mutifractal analysis is a powerful tool to describe the physical processes underlying nitrogen adsorption and desorption, and in this respect goes beyond parameters such as SSA, based on classical statistics. Thus, multifractal analysis offer additional information of value as it reveals the hidden structure of adsorption and desorption isotherms. The choice of representing soil properties in terms of nonlinear process provide new insight for interpretation of the phenomena studied. In this perspective the information obtained could be useful for soil quality evaluations, based on inherent soil properties.

In our study, multifrcatal analysis was used to evaluate N_2 isotherms from two contrasting soil groups. However, for a horizon with a given texture, management system has been proven to influence SSA and multifractal characteristics of adsorption isotherms, as well (Paz Ferreiro et al., 2009). This suggests further analysis of N_2 adsorption and desorption isotherms from the topsoil horizon of a loamy textured or a clayey textured soil under different management systems could be useful for assessment of environmentally sound practices in the studied landscapes.

Conclusions

For all the collected samples, SSA showed a strong correlation with clay content. However, no significant relationship was found between these soil surface properties and properties of the soil exchangeable complex.

Nitrogen adsorption and desorption isotherms exhibited multifractal behaviour. However, adsorption isotherms were less evenly distributed measures than desorption isotherms, as indicated by lower entropy dimension, D_1. Also adsorption isotherms were more heterogeneous than desorption isotherms, as the former exhibited higher widths of generalized dimension ($D_{-5} - D_5$) and singularity spectra(α_{max}- α_{min}) than the later. Accordingly, multifractal parameters from adsorption and desorption isotherms were quite different. Contrasting multifractal behaviour of NAIs and NDIs proved to be mainly related to the characteristics of the hysteretic loop.

Several multifractal parameters extracted from NAIs and NDIs also were useful to distinguish between the medium textured and clayey soils. Moreover, in opposite to previous work, there was no significant relationship between multifractal parameters from adsorption and desorption isotherms and soil textural fractions or soil organic carbon content. Altogether, multifractal analysis of NAIs and NDIs provided new information for describing the surface-pore interface of soils in terms of nonlinear processes.

Acknowledgements. This work was supported by Spanish Ministry of Science and Technology (project CGL2013-47814-C2) and by Xunta de Galicia (project 10MRU162037PR).

REFERENCES

Bartoli, F., Poulenard, A. J., and Schouller, B. E.: Influence of allophane and organic matter contents on surface properties of Andosols, Eur. J. Soil Sci., 58, 450-464, 2007.

Brunauer, S., Emmett, P. H., and E. Teller, E.: Adsorption of gases in multimolecular layers, J. Am. Chem. Soc., 60, 309-319, 1938.

Broekhoff, J. C. P., and de Boer, J. H.: Pore systems in catalysts. XI. Pore distribution calculations from the adsorption branch of a nitrogen adsorption isotherm in the case of “ink-bottle” type pores, J. Catal., 10 (2), 153-165, 1968a.

Broekhoff, J. C. P. and J. H de Boer, J. H.: Pore systems in catalysts. XII. Pore distributions from the desorption branch of a nitrogen sorption isotherm in the case of cylindrical pores. 1. An analysis of the capillary evaporation process, J. Catal., 10 (4), 391-400, 1968b.

Carter, D.L., Mortland, M. M., and Kemper, W. D.: Specific surface, In A. Klute (ed.), *Methods of soil analysis*, 2nd ed, Agron. Monogr. 9., ASA and SSSA, Madison, WI, pp. 413-423, 1986.

Carter, , M. R., Gregorich, E. G., Anderon, D. W., Doran, J. W., Janzen, H. H., and Pierce, F. J.: Concepts of soil quality and their significance, In: Gregorich, E. G. and Carter, M. R. (eds), *Soil Quality for crop Production and Ecosystem Health*, Elsevier. Ansterdam, pp 1-19, 1997.

Chhabra A. B., and Jensen, R, V.: Direct determination of the f(α) singularity spectrum, Phys. Rev. Lett., 62, 1327-1330, 1989.

Doran, J. W., and T. B.Parkin, B. T.: Defining and assessing soil quality, In: Doran, J. W., Coleman, D. C., Bezedick, D. F., and Stewart, B. A. (eds), *Defining Soil Quality for a Sustainable Environment*, Special Publcation nº 35, ASA, Madison, WI, pp 3-21, 1994.

EMBRAPA (Brazilian Agricultural Research Corporation).: Methods of soil analysis manual. (In Portuguese), 2nd Edition. Río de Janeiro, Brazil. 212 pp, 1997.

EMBRAPA (Brazilian Agricultural Research Corporation).: Brazilian System of Soil Classification. (In Portuguese), Brasilia, Brazil. 412 pp, 2006..

Feller, C., Shouller, E., Thomas F., Rouiller, J., and Herbillon, A. J.: N_2-BET specific surface areas of some low activity clay soils and their relationships with secondary constituents and organic matter contents. Soil Sci., 153, 293-299, 1992.

Hajnos, M., Korsunskaia, L., and. Pachepsky, Y.: Soil pore surface properties in managed grasslands, Soil Till. Res., 55, 63-70, 2000.

Halsey, T.C., Jensen, M. H., Kanadoff, L. P., Procaccia, I., and Shraiman, B. I.: Fractal measures and their singularities: The characterization of strange sets, Phys. Rev. A, 33, 1141-1151, 1986.

Hepper, E. N., Buschiazzo, D. E., Hevia, G. C., Urioste, A., and Antón, L.: Clay mineralogy, cation exchange capacity and specific surface area of loess soils with different volcanic ash contents, Geoderma, 135:216-223, 2006.

IPT. (Institute for Technological Research of São Paulo State).: Geological map of São Paulo State, V.2, scale 1:500.000. (In Portuguese), Pro-Mineiro, SP, Brazil, 126 pp, 1981.

IPT. (Institute for Technological Research of São Paulo State).: Geomorfological map of São Paulo State, V.1, scale 1:500.000. (In Portuguese), USP, SP, Brazil, 1997.

Jozefaciuk, G., Toth, T., and Szendrei, G.: Surface and micropore properties of saline soil profiles. Geoderma 135, 1-15, 2006.

Lado, M., Borisover, M., and Paz González, A.: Multifractal analysis of nitrogen adsorption isotherms obtained from organoclays exposed to different temperatures. Vadose Zone Journal, 12, 3. DOI: 10.2136/vzj2012.0206, 2013.

Lal, R.: Soil erosion impact on agronomic productivity and environmental quality. Critical Reviews in Plant Science, 17, 943-950, 1998.

Miranda, J. G. V., Montero, E., Alves, M. C., Paz González, A., and Vidal Vázquez, E.: Multifractal characterization of saprolite particle-size distributions after topsoil removal, Geoderma ,134, 373-385, 2006.

Oliveira, J. B., J. R. F. Menk and C. L. Rotta.: Report on semi-detailed pedological survey of soils from São Paulo state. Grid of Campinas. Rio de Janeiro, Supren, Abge, 1979.

Pachepsky, Y., Polubesova, T. A., Hajnos, M., Sokolowska, Z., and Józefaciuk, G., Fractal parameters of pore surface area as influenced by simulated soil degradation, Soil Sci. Soc. Am. J., 59, 68-75, 1995.

Paz-Ferreiro, J., Wilson, M., and Vidal Vázquez. E.: Multifractal description of nitrogen adsorption isotherms, Vadose Zone J., 8,209-219, 2009.

Paz-Ferreiro, J., Miranda, J. G. V., and Vidal Vázquez, E.: Multifractal analysis of soil porosity based on mercury injection and nitrogen adsorption, Vadose Zone J., 9, 325-335, 2010.

Paz-Ferreiro, J., da Luz, L.R.Q.P., Lado, M., and Vidal Vázquez, E.: Specific surface area and multifractal parameters of associated nitrogen adsorption and desorption isotherms in soils from Santa Catarina, Brazil, Vadose Zone Journal, 12 (3), doi:10.2136/vzj2012.0203, 2013.

Petersen, L.W., Moldrup, P., Jacobsen, O. H., and Rolston, D. E.: Relations between specific surface area and soil physical and chemical properties, Soil Sci., 16, 9-21, 1996.

Posadas, A. N. Giménez, D. D., Quiroz, R., and Protz, R.: Multifractal characterization of soil pore systems, Soil Sci. Soc. Am. J., 67,1361-1369, 2003.

Rouquerol, F., Rouquerol, J., and Sing. K.: Adsorption by powders and porous solids. Academic Press, London, 1999.

SAS-Statistical Analysis System, SAS Institute.: Users SAS Institute. NC. USA, 1999.

Soil Survey Staff.: Key to soil taxonomy, 11th Edition, Natural Resources Conservation Service, Washington, DC, 338 pp, 2010.

Sokolowska, Z., Hajinos, M., Hoffman, C., Rengar, M., and Sokolowski, S.: Surface fractal dimension of thermally treated peat soils from adsorption isotherms of nitrogen, J. Plant Nutr, Soil Sci., 163, 441-446, 2001.

Tarquis, A. M., McInnes, K. J., Key. J. R, Saa, A., García, M. R., and Diaz, M. C.: Multiscaling analysis in a structured clay soil using 2D images, J. Hydrol., 322, 236-246, 2006.

Van Raij, B., J. de Andrade, C., Cantarella, H., and Quaggio, J. A.: Chemical analysis for evaluation of tropical soils fertility, Instituto Agronômico, Campinas, Brazil, 284 pp, 2001.

Vidal Vázquez, E., García Moreno, R., Miranda, J.G.V., Díaz, M.C., Saa Requejo, A., Paz-Ferreiro, J., and Tarquis, A.M.: Assessing soil surface roughness decay during simulated rainfall by multifractal analysis., Nonlin. Proc. in Geophysics, 15, 457–468, 2008.

Vidal-Vázquez, E. and Paz-Ferreiro, J.: Multifractal characteristics of nitrogen adsorption isotherms from tropical soils, Soil Sci., 42, 131-13, 2012.

WRB (World Reference Base for Soil Resources).: A framework for international classification, correlation and communication 2006. World Soil Resources Reports, Nº 103, FAO, Rome, 127 pp, 2006.

Table 1.- General information about the studied samples: horizon, vertical limits, location, altitude, parent material, and classification following Brazilian System of Soil Classification (BSSC), Soil Survey Staff (SSS) and World Reference Base (WRB).

Soil	Horizon	Depth/cm	Location	Parent Material	BSSC	SSS	WRB	Texture
1	Ap	0-8	Monte Mor (607 m)	Sandstone	Neossolo	*Typic*	Leptosol	loam
	C1	8-20	22^{o}55’15.71’’S	and silt	Regolítico	*Udorthent*		loam
	C2	20-32	47^{o}17’09,06’’W					loam
2	Ap1	0-13	Monte Mor (610 m)	Sandstone	Argissolo	*Typic*	Acrisol	loam
	Ap2	13-25	22^{o}55’06.64’’S	and silt	Amarelo	*Hapludult*		sandy loam
	AB	25-37	47^{o}16’59.71’’W		Distrófico			sandy loam
	Bt	37-54						sandy loam
	Bt/Cr1	54-78						loam
3	Ap1	0-15	Monte Mor (622m)	Sandstone	Argissolo	*Arenic*	Acrisol	sandy loam
	Ap2	15-30	22^{o}54’26.97’’S	and silt	Vermelho	*Hapludult*		sandy loam
	A2/ E	30-42	47^{o}17’12.78’’W		Amarelo			sandy loam
	E	42-62			Distrófico			sandy loam
	Bt	62-92						loam
	Bt/Cr	+ 92						loam
4	Ap1	0-20	Sumaré (640 m)	Weathered material	Latossolo	*Humic*	Ferralsol	loam
	Ap2	20-40	22^{o}52’21.04’’S	from basic rocks	Vermelho	*Hapludox*		sandy clay
	A21	40-70	47^{o}18’18.69’’W	(Diabase)	Amarelo			clay
	A22	70-100			Distrofico			clay
	A23	100-130			húmico			clay
	A24	130-150						clay
	A25	150-180						clay
	Bw1	250-300						clay
5	Ap	0-10	Sumaré (574 m)	Weathered material	Nitossolo	*Typic*	Nitisol	clay
	B1	10-35	22^{o}47’33.58’’S	from clayey and	Vermelho	*Rhodudult*		clay
	B21	35-60	47^{o}20’1.64’’W	loamy sediments	Distroférrico			clay

	B22	60-76			típico			clay
	B23	76-104						clay
6	Ap	0-18	Campinas (620 m)	Weathered material	Latossolo	*Rhodic*	Ferralsol	clay
	AB	18-36	22°49’11’’S	from basic rocks	Vermelho	*Hapludox*		clay
	Bw1	36-73	47°03’43’’W	(Diabase)	Distroférrico			clay
	Bw2	73-117			típico			clay
	Bw3	117-158						clay

Table 2. Correlation matrix for sand, silt, clay, organic matter content (OM), pH, complex exchange properties and surface properties

	Sand	Silt	Clay	OM	pH	H + Al	SB	CEC	V	SSA
Sand	1									
Silt	0.406*	1								
Clay	-0.892**	-0.775**	1							
OM	-0.235	0.077	0.124	1						
pH	-0.689**	0.045	0.454**	0.032	1					
H + Al	0.113	-0.529**	0.183	0.322	-0.622**	1				
SB	-0.557**	0.280	0.247	0.481**	0.700**	-0.464**	1			
CEC	-0.098	-0.480**	0.305	0.555**	-0.415*	0.934**	-0.116	1		
V	-0.438*	0.404*	0.103	0.110	0.835**	-0.783**	0.866*	-0.529**	1	
SSA	-0.878**	-0.779**	0.992**	0.087	0.436*	0.185	0.239	0.303	0.101	1

(* and **, correspond to $P < 0.05$ and $P < 0.01$, respectively)

Abbreviations: (H+Al = exchangeable H + Al, SB = sum of exchangeable base, i.e., K+ Mg+ Ca, CEC = cation exchange capacity, V = percent base saturation, SSA = specific surface area and $V_{0.95}$= cumulative N_2 volume adsorbed at 0.95 relative pressure)

Table 3.- Multifractal parameters extracted from the generalized dimension function (D_{-5}, D_1, D_2, D_5) and from the singularity spectrum (α_0) of nitrogen adsorption isotherms.(NAIs).

Horizon/depth	D_{-5}	D_1	D_2	D_5	α_0
Typic Udorthent					
Ap (0-8)	2.309 ± 0.346	0.521 ± 0.036	0.343 ± 0.035	0.229 ± 0.022	1.500 ± 0.016
C1 (8-20)	1.397 ± 0.170	0.568 ± 0.028	0.397 ± 0.028	0.267 ± 0.020	1.320 ± 0.027
C2 (20-32)	2.366 ± 0.334	0.513 ± 0.018	0.390 ± 0.020	0.261 ± 0.015	1.509 ± 0.029
Typic Hapludult					
Ap1 (0-13)	1.999 ± 0.289	0.568 ± 0.043	0.403 ± 0.045	0.276 ± 0.033	1.439 ± 0.019
Ap2 (13-25)	1.168 ± 0.122	0.615 ± 0.037	0.461 ± 0.043	0.319 ± 0.033	1.266 ± 0.027
AB (25-37)	1.168 ± 0.118	0.621 ± 0.034	0.469 ± 0.040	0.325 ± 0.031	1.260 ± 0.025
Bt (37-54)	1.517 ± 0.262	0.642 ± 0.042	0.534 ± 0.061	0.388 ± 0.052	1.326 ± 0.027
Bt/Cr1 (54-78)	1.274 ± 0.203	0.643 ± 0.035	0.523 ± 0.050	0.373 ± 0.041	1.280 ± 0.021
Arenic Hapludult					
Ap1 (0-15)	2.051 ± 0.310	0.505 ± 0.038	0.313 ± 0.032	0.208 ± 0.022	1.462 ± 0.023
Ap2 (15-30)	1.547 ± 0.181	0.523 ± 0.044	0.349 ± 0.045	0.235 ± 0.029	1.916 ± 0.017
A2/ E (30-42)	2.357 ± 0.379	0.531 ± 0.043	0.360 ± 0.042	0.243± 0.030	1.522 ± 0.021
E (42-60)	2.169 ± 0.338	0.524 ± 0.041	0.356 ± 0.041	0.240 ± 0.029	1.495 ± 0.020
Bt (62-92)	1.148 ± 0.123	0.596 ± 0.044	0.427 ± 0.048	0.294 ± 0.036	1.278± 0.032
Bt/Cr (>92)	1.421 ± 0.209	0.548 ± 0.041	0.374 ± 0.042	0.253 ± 0.031	1.357± 0.031
Mean group 1	**1.986**	**0.566**	**0.407**	**0.279**	**1.424**
Humic Hapludox					
Ap1 (0-20)	2.710 ± 0.378	0.579 ± 0.071	0.461 ± 0.092	0.345 ± 0.081	1.547± 0.016
Ap2 (20-40)	2.581 ± 0.364	0.609 ± 0.074	0.512 ± 0.110	0.410 ± 0.111	1.518 ± 0.025
A21 (40-70)	2.261 ± 0.314	0.597 ± 0.066	0.482 ± 0.092	0.366 ± 0.085	1.478 ± 0.028
A22 (70-100)	2.385 ± 0.334	0.559 ± 0.060	0.420 ± 0.072	0.298 ± 0.057	1.515 ± 0.026
A23 (100-130)	2.642 ± 0.381	0.585 ± 0.076	0.475 ± 0.105	0.367 ± 0.098	1.534 ± 0.030
A24 (130-150)	2.847 ± 0.423	0.567 ± 0.069	0.440 ± 0.087	0.325 ± 0.075	1.571 ± 0.026
A25 (150-180)	2.904 ± 0.463	0.554 ± 0.063	0.412 ± 0.073	0.292 ± 0.058	1.568 ± 0.028
Bw1 (250-300)	2.566 ± 0.430	0.565 ± 0.063	0.423 ± 0.075	0.301 ± 0.060	1.518 ± 0.038
Typic Rhodudult					
Ap (0-10)	2.514 ± 0.423	0.580 ± 0.057	0.441 ± 0.069	0.314 ± 0.056	1.511 ± 0.033
B1 (10-35)	2.346 ± 0.364	0.562 ± 0.057	0.413 ± 0.066	0.290 ± 0.052	1.485 ± 0.031
B21 (35-60)	2.556 ± 0.392	0.565 ± 0.059	0.419 ± 0.068	0.295 ± 0.053	1.514 ± 0.027
B22 (60-76)	2.632± 0.415	0.578 ± 0.059	0.439 ± 0.071	0.313 ± 0.057	1.505 ± 0.031
B23 (76-104)	2.914 ± 0.514	0.529 ± 0.061	0.376 ± 0.069	0.265 ± 0.054	1.578 ± 0.037
Rhodic Hapludox					
Ap (0-18)	2.418 ± 0.384	0.602 ± 0.064	0.482 ± 0.084	0.356 ± 0.072	1.484 ± 0.030
AB (18-36)	2.402 ± 0.360	0.579 ± 0.061	0.442 ± 0.073	0.316 ± 0.059	1.497 ± 0.027
Bw1 (36-73)	2.670 ± 0.415	0.593 ± 0.068	0.474 ± 0.091	0.358 ± 0.083	1.513 ± 0.032
Bw2 (73-117)	2.438 ± 0.394	0.578 ± 0.065	0.444 ± 0.080	0.321 ± 0.067	1.494 ± 0.035
Bw3 (117-158)	2.557 ± 0.423	0.580 ± 0.069	0.455 ± 0.090	0.339 ± 0.079	1.508 ± 0.036
Mean group 2	**1.998**	**0.576**	**0.445**	**0.288**	**1.519**

Table 4.- Multifractal parameters extracted from the generalized dimension function (D_{-5}, D_1, D_2, D_5) and from the singularity spectrum (α_0) of nitrogen desorption isotherms.(NDIs)

Horizon/depth	D_{-5}	D_1	D_2	D_5	α_0
Typic Udorthent					
Ap (0-8)	1.546 ± 0.065	0.678 ± 0.013	0.528 ± 0.027	0.370 ± 0.027	1.257 ± 0.002
C1 (8-20)	1.401 ± 0.044	0.708 ± 0.014	0.613 ± 0.031	0.451 ± 0.029	1.204 ± 0.009
C2 (20-32)	1.388 ± 0.056	0.675 ± 0.014	0.610 ± 0.026	0.435 ± 0.035	1.198 ± 0.013
Typic Hapludult					
Ap1 (0-13)	1.755± 0.169	0.720 ± 0.022	0.628 ± 0.047	0.474 ± 0.050	1.257 ± 0.004
Ap2 (13-25)	1.257 ± 0.046	0.757 ± 0.034	0.683 ± 0.066	0.538 ± 0.078	1.148 ± 0.017
AB (25-37)	1.256 ± 0.049	0.762 ± 0.031	0.696 ± 0.063	0.551 ± 0.077	1.142 ± 0.015
Bt (37-54)	1.187 ± 0.039	0.797 ± 0.035	0.769 ± 0.073	0.665 ± 0.101	1.115 ± 0.016
Bt/Cr1 (54-78)	1.216 ± 0.052	0.797 ± 0.031	0.786 ± 0.067	0.686 ± 0.096	1.114 ± 0.014
Arenic Hapludult					
Ap1 (0-15)	1.245 ± 0.054	0.620 ± 0.053	0.439 ± 0.069	0.310 ± 0.058	1.241 ± 0.033
Ap2 (15-30)	1.301 ± 0.067	0.640 ± 0.053	0.483 ± 0.075	0.349 ± 0.066	1.242 ± 0.028
A2/ E (30-42)	1.277 ± 0.068	0.648 ± 0.054	0.496 ± 0.077	0.362 ± 0.069	1.224 ± 0.029
E (42-60)	1.218 ± 0.061	0.660 ± 0.048	0.503 ± 0.069	0.362 ± 0.061	1.212 ± 0.029
Bt (62-92)	1.174 ± 0.051	0.723 ± 0.059	0.625 ± 0.102	0.524 ± 0.123	1.172 ± 0.031
Bt/Cr (>92)	1.227 ± 0.053	0.678 ± 0.058	0.554 ± 0.094	0.431 ± 0.097	1.203 ± 0.031
Mean group 1	**1.318**	**0.704**	**0.601**	**0.465**	**1.195**
Humic Hapludox					
Ap1 (0-20)	0.851 ± 0.032	0.653 ± 0.048	0.494 ± 0.059	0.350 ± 0.048	1.224 ± 0.033
Ap2 (20-40)	0.850 ± 0.036	0.664 ± 0.039	0.496 ± 0.046	0.347 ± 0.033	1.213 ± 0.029
A21 (40-70)	0.872 ± 0.036	0.650 ± 0.038	0.474 ± 0.043	0.327± 0.036	1.217 ± 0.029
A22 (70-100)	0.793 ± 0.033	0.666 ± 0.057	0.526 ± 0.072	0.399 ± 0.080	1.220 ± 0.035
A23 (100-130)	0.858 ± 0.035	0.638 ± 0.047	0.468 ± 0.056	0.327 ± 0.064	1.228 ± 0.034
A24 (130-150)	0.840 ± 0.035	0.644 ± 0.050	0.480 ± 0.062	0.340 ± 0.070	1.228 ± 0.035
A25 (150-180)	0.851 ± 0.039	0.642 ± 0.051	0.479 ± 0.054	0.340 ± 0.052	1.229 ± 0.034
Bw1 (250-300)	0.785 ± 0.031	0.666 ± 0.059	0.516 ± 0.064	0.380 ± 0.072	1.217 ± 0.036
Typic Rhodudult					
Ap (0-10)	0.705 ± 0.040	0.709 ± 0.061	0.602 ± 0.098	0.485 ± 0.105	1.194 ± 0.032
B1 (10-35)	0.756 ± 0.033	0.678 ± 0.063	0.544 ± 0.083	0.418 ± 0.091	1.207 ± 0.035
B21 (35-60)	0.793 ± 0.040	0.670 ± 0.059	0.529 ± 0.065	0.396 ± 0.079	1.212 ± 0.034
B22 (60-76)	0.794 ± 0.037	0.676 ± 0.050	0.525 ± 0.055	0.378 ± 0.065	1.201 ± 0.032
B23 (76-104)	0.695 ± 0.037	0.661 ± 0.077	0.542 ± 0.078	0.468 ±0.135	1.226 ± 0.041
Rhodic Hapludox					
Ap (0-18)	0.807 ± 0.039	0.680 ± 0.045	0.531 ± 0.049	0.384 ± 0.051	1.202 ± 0.029
AB (18-36)	0.737 ± 0.031	0.691 ± 0.061	0.570 ± 0.092	0.445 ± 0.072	1.202 ± 0.034
Bw1 (36-73)	0.756 ± 0.039	0.687 ± 0.054	0.554 ± 0.077	0.420 ± 0.093	1.202 ± 0.033
Bw2 (73-117)	0.830 ± 0.037	0.656 ± 0.047	0.488 ± 0.049	0.343 ± 0.053	1.212 ± 0.033
Bw3 (117-158)	0.834 ± 0.037	0.650 ± 0.051	0.488 ± 0.063	0.347 ± 0.071	1.217 ± 0.034
Mean group 2	**1.183**	**0.666**	**0.517**	**0.383**	**1.214**

Table 5.- Mean values of multifractal parameters from N_2 adsorption and desorption isotherms for the two studied soil groups, and one way ANOVA analysis.

	D_{-5}	D_1	D_2	D_5	$(D_{-5} - D_5)$	α_0
	Adsorption (NAI)					
Group 1	1.986	0.563	0.405	0.279	1.706	1.396
Group 2	2.575	0.576	0.445	0.326	2.249	1.519
Fvalue	12.598	0.857	4.648	8.645	19.148	21.460
p*	**0.001**	0.362	**0.039**	**0.006**	**0.000**	**0.000**
	Desorption (NDI)					
Group 1	1.318	0.704	0.601	0.465	0.853	1.195
Group 2	1.183	0.666	0.517	0.383	0.800	1.214
F value	25.762	7.361	9.731	7.377	0.966	2.528
p*	**0.000**	**0.011**	**0.004**	**0.011**	0.334	0.122

(Group 1 are medium textured soils (P1, P2 and P3), and group 2 are heavy textured soils (P4.P5 and P6) * bold indicate that the results are significantly different ($P < 0.05$))

Captions to figures

Figure 1. Examples of Nitrogen adsorption-desorption isotherms for samples from two horizons with contrasting texture (Profile 1, horizon Ap and Profile 6 , horizon Ap).

Figure 2.- Relationship between clay content and SSA for all the horizons of horizons studied.

Figure 3.- Examples of singularity spectra for adsorption isotherms (NAIs) of soil horizons with contrasting texture (Profile 1, horizons Ap and C1 and profile 6, horizons Ap and AB). Captions A and B in the legend indicate two repetitions per sample.

Figure 4.- Examples of singularity spectra for desorption isotherms (NDIs) of soil horizons with contrasting texture (Profile 1, horizons Ap and C1 and profile 6, horizons Ap and AB). Captions A and B in the legend indicate two repetitions per sample.

Figure 5.- Relationships between entropy dimension, D_1, from N_2 adsorption and desorption isotherms. (P1-P3 = soils over sandstone poor in bases, P1-P3 = soils over basic parent material).

Figure 1

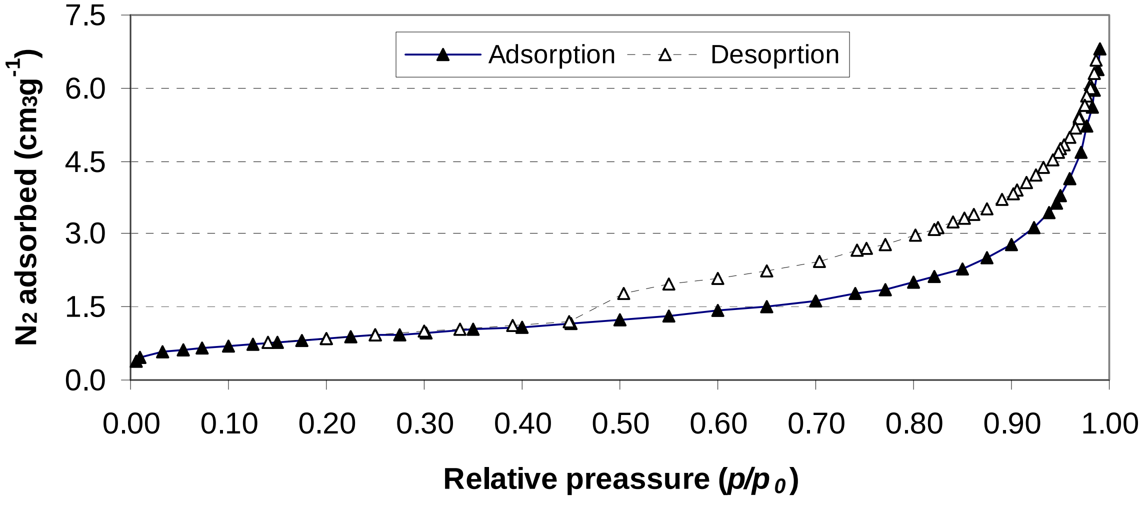

Profile 1, Typic Udorthent, horizon Ap, 125 g kg^{-1} clay

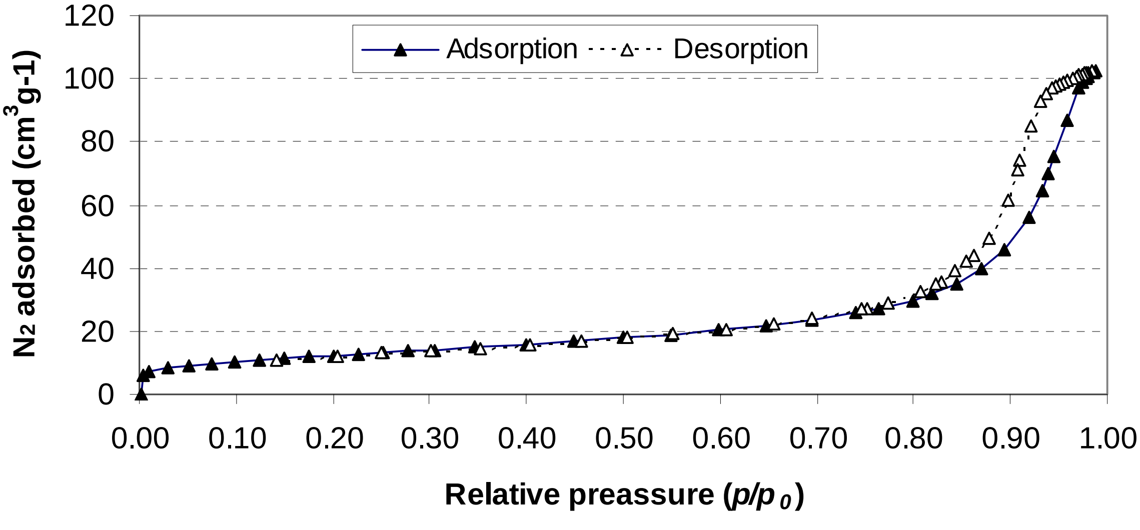

Profile 6, Rodic Hapludox, horizon Ap, 573 g kg^{-1} clay

Figure 2

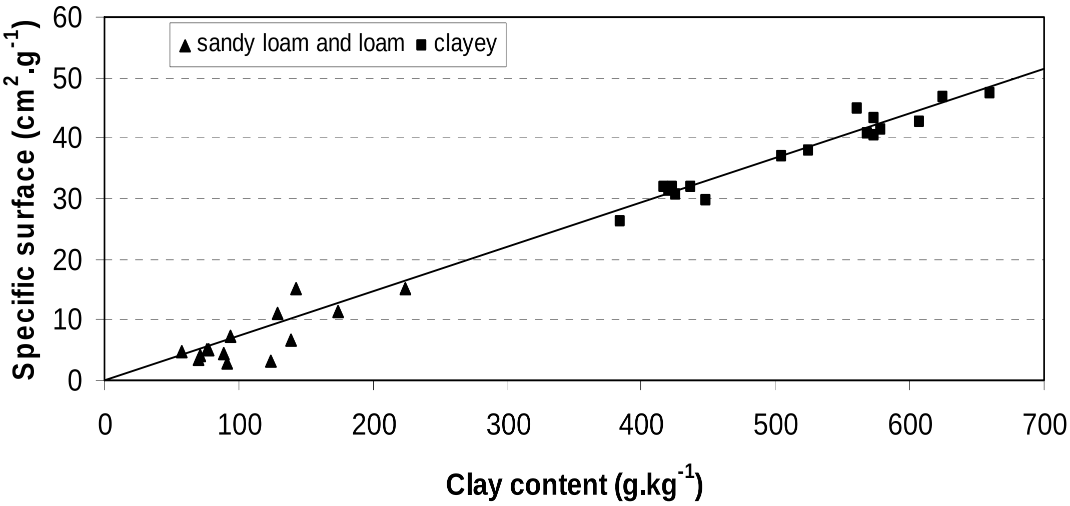
sandy loam and loam
clayey
Specific surface (cm2.g-1)
Clay content (g.kg-1)
0
10
20
30
40
50
60
0
100
200
300
400
500
600
700

Figure 3

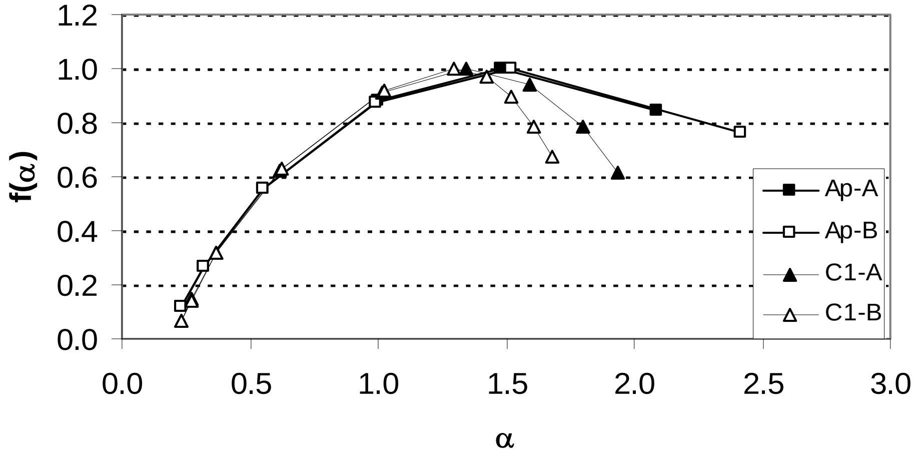

Profile 1, Typic Udorthent, horizons Ap and C1

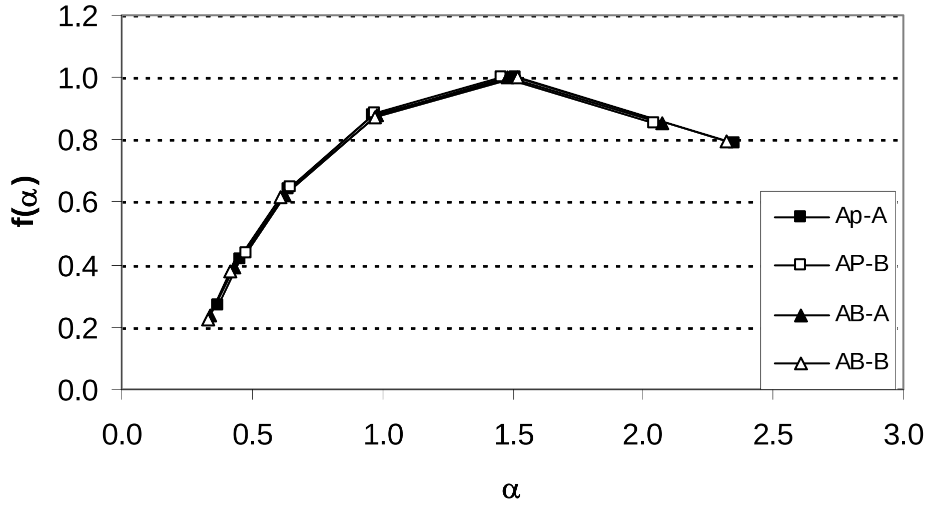

Profile 6, Rodic Hapludox, horizons Ap and AB

Figure 4

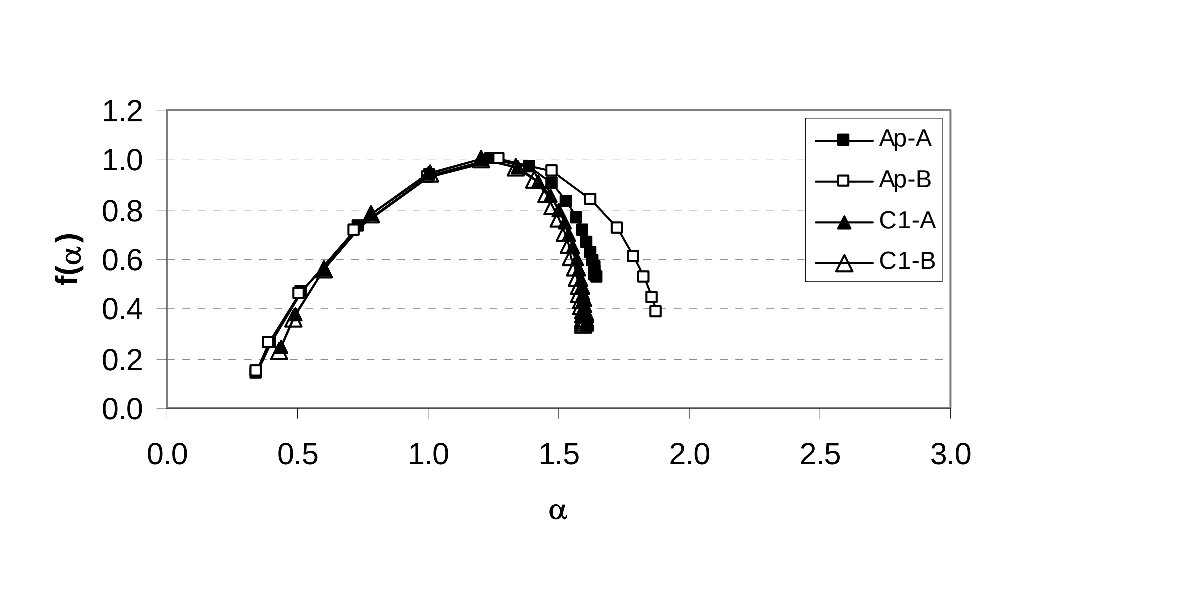

Profile 1, Typic Udorthent, horizons Ap and C1

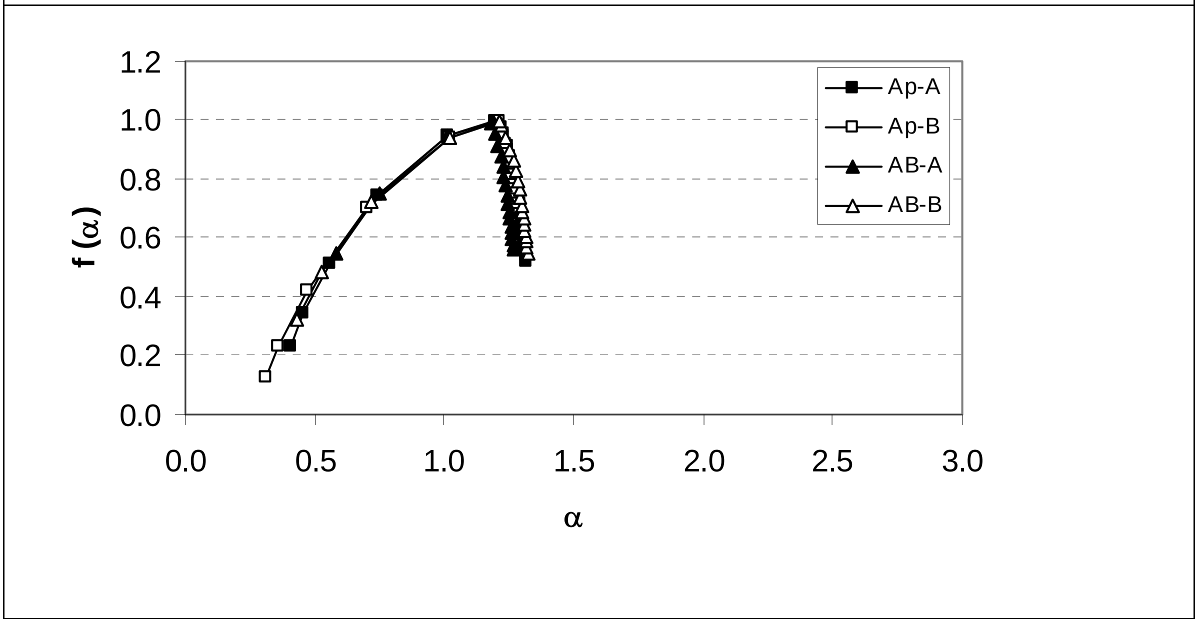

Profile 6, Rodic Hapludox, horizons Ap and AB

Figure 5

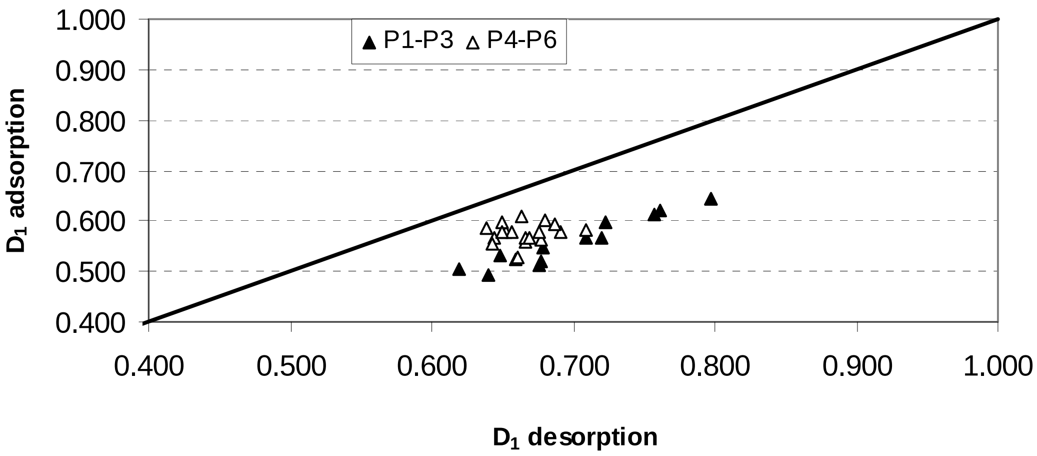
P1-P3
P4-P6
D1 adsorption
D1 desorption
1.000
0.900
0.800
0.700
0.600
0.500
0.400
0.400
0.500
0.600
0.700
0.800
0.900
1.000